GENE THERAPY

Preclinical modeling highlights the therapeutic potential of hematopoietic stem cell gene editing for correction of SCID-X1

Giulia Schiroli,[1,2] Samuele Ferrari,[1,2] Anthony Conway,[3] Aurelien Jacob,[1] Valentina Capo,[1] Luisa Albano,[1] Tiziana Plati,[1] Maria C. Castiello,[1] Francesca Sanvito,[4] Andrew R. Gennery,[5] Chiara Bovolenta,[6] Rahul Palchaudhuri,[7,8] David T. Scadden,[8] Michael C. Holmes,[3] Anna Villa,[1,9] Giovanni Sitia,[10] Angelo Lombardo,[1,2] Pietro Genovese,[1]*† Luigi Naldini[1,2]*†

Targeted genome editing in hematopoietic stem/progenitor cells (HSPCs) is an attractive strategy for treating immunohematological diseases. However, the limited efficiency of homology-directed editing in primitive HSPCs constrains the yield of corrected cells and might affect the feasibility and safety of clinical translation. These concerns need to be addressed in stringent preclinical models and overcome by developing more efficient editing methods. We generated a humanized X-linked severe combined immunodeficiency (SCID-X1) mouse model and evaluated the efficacy and safety of hematopoietic reconstitution from limited input of functional HSPCs, establishing thresholds for full correction upon different types of conditioning. Unexpectedly, conditioning before HSPC infusion was required to protect the mice from lymphoma developing when transplanting small numbers of progenitors. We then designed a one-size-fits-all *IL2RG* (interleukin-2 receptor common γ-chain) gene correction strategy and, using the same reagents suitable for correction of human HSPC, validated the edited human gene in the disease model in vivo, providing evidence of targeted gene editing in mouse HSPCs and demonstrating the functionality of the *IL2RG*-edited lymphoid progeny. Finally, we optimized editing reagents and protocol for human HSPCs and attained the threshold of *IL2RG* editing in long-term repopulating cells predicted to safely rescue the disease, using clinically relevant HSPC sources and highly specific zinc finger nucleases or CRISPR (clustered regularly interspaced short palindromic repeats)/Cas9 (CRISPR-associated protein 9). Overall, our work establishes the rationale and guiding principles for clinical translation of SCID-X1 gene editing and provides a framework for developing gene correction for other diseases.

INTRODUCTION

Targeted genome editing may enhance the precision of genetic engineering in cell and gene therapy. It exploits artificial nucleases, such as zinc finger nucleases (ZFNs), transcription activator-like effector nucleases (TALENs), and RNA-based CRISPR (clustered regularly interspaced short palindromic repeats)/Cas9 (CRISPR-associated protein 9) nucleases, to target a DNA double-strand break (DSB) or nick into a predetermined sequence of the genome (*1*, *2*). Depending on the DSB repair pathway engaged, the outcome may be functional inactivation of the targeted locus by nonhomologous end joining (NHEJ), which often introduces small insertions or deletions ("indels"), or introduction of a new sequence by homology-directed repair (HDR) from an exogenous template DNA bearing homology to the sequences flanking the DSBs. The latter strategy has been used to knock in exogenous gene sequences, such as functional complementary DNA (cDNA), into inherited defective genes downstream of their own promoter, thus reconstituting the function and endogenous expression control of the mutant gene, without the risk of random insertional mutagenesis (*3*–*6*). Moreover, this approach has the advantage that most disease-causing mutations affecting the locus, including deletions, can be treated with the same engineered nucleases.

Notwithstanding the therapeutic potential of gene editing for the treatment of immune hematological diseases, a major challenge to its application comes from the limited efficiency of HDR in hematopoietic stem/progenitor cells (HSPCs). Despite recent reports of improvements in ex vivo gene editing protocols for human (*7*–*11*) and nonhuman primate HSPCs (*12*), HDR-mediated insertion of exogenous genes remains constrained in long-term severe combined immunodeficiency (SCID)–repopulating HSPCs (*7*–*11*), likely because of low expression of the HDR machinery, cell quiescence, induced differentiation or apoptosis in response to DNA DSBs, and limited uptake of template DNA. A limited yield of edited hematopoietic stem cells (HSCs) may affect the feasibility and safety of clinical development of gene editing. Moreover, stem cell–based therapeutics will require highly specific targeted gene editing, which might be achieved with new or improved nuclease platforms.

We have been developing a gene editing strategy to correct mutations in the interleukin-2 receptor common γ-chain (*IL2RG*) gene, which are responsible for X-linked SCID (SCID-X1) (*13*), by knocking in a corrective cDNA into the affected locus (*7*). Although we have shown expression of a functional IL2RG from the edited allele in human HSPCs (*7*), it remains unknown whether the edited locus fully recapitulates the physiological gene expression pattern and its function during cell differentiation and in orchestrating an immune response in vivo. The knock-in strategy may fail to preserve or rescue some fine regulatory features associated with transcription and/or alternative splicing of intronic sequences not included within the corrective cDNA or induce

[1]San Raffaele Telethon Institute for Gene Therapy, 20132 Milan, Italy. [2]Vita-Salute San Raffaele University, 20132 Milan, Italy. [3]Sangamo Therapeutics, Richmond, CA 94804, USA. [4]Pathology Unit, Department of Oncology, San Raffaele Scientific Institute, 20132 Milan, Italy. [5]Institute of Cellular Medicine, Newcastle University, Newcastle upon Tyne NE2 4HH, UK. [6]MolMed S.p.A., 20132 Milan, Italy. [7]Magenta Therapeutics, Cambridge, MA 02139, USA. [8]Harvard Stem Cell Institute, Cambridge, MA 02138, USA. [9]National Research Council, Institute of Genetic and Biomedical Research Milan Unit, 20138 Milan, Italy. [10]San Raffaele Scientific Institute, 20132 Milan, Italy.
*These authors contributed equally to this work.
†Corresponding author. Email: genovese.pietro@hsr.it (P.G.); naldini.luigi@hsr.it (L.N.)

an epigenetic memory of the DNA repair, which may affect gene regulation. Moreover, it remains unclear whether a low input of edited progenitors can safely and effectively rescue the disease, even in the presence of the growth advantage conferred by gene correction. Thus, there is a need to develop stringent preclinical models of disease correction by HSPC gene editing that suitably interrogate the features of the therapeutic cell product and its administration strategy, two parameters that may affect the timing and extent of immune reconstitution.

RESULTS

Establishing the threshold proportion of functional HSPCs required for immune reconstitution

To model SCID-X1 gene correction, we developed a mouse model carrying the human *IL2RG* gene with a disease-causing mutation (R226H), which abrogates γ-chain expression (*13*), in place of the murine *Il2rg* gene (fig. S1A). By immunophenotypical and histological characterization, we found that these humanized SCID-X1 mice had impairments in lymphoid development that phenocopy those reported for *Il2rg*$^{-/-}$ mice (figs. S1 and S2 and table S1) (*14*–*16*).

We then determined the lowest fraction of functional HSPCs required to rescue the immune function of SCID-X1 mice. We performed competitive transplantations with wild-type (WT) and *IL2RG*$^{-/-}$ HSPCs mixed at different ratios in SCID-X1 recipients conditioned by total body irradiation (TBI) and monitored lymphohematopoietic reconstitution over time (Fig. 1A). We found that B and T cells derived almost completely from WT cells, even in mice transplanted with the lowest fraction (1%) of functional HSPCs, demonstrating their strong selective advantage over defective cells. Selective advantage was also found within the Lin$^-$Sca1$^+$ bone marrow (BM) cells, which include progenitors endowed with lymphoid potential (fig. S3A) (*17*). Conversely, the WT chimerism observed within mature myeloid cells in the peripheral blood (PB), myeloid progenitors, and the more primitive KLS$^+$ (Kit$^+$Lin$^-$ Sca1$^+$) cells closely mirrored those of the input HSPC, as expected for cell types that are not dependent on IL2RG signaling for their survival and proliferation (Fig. 1B and fig. S3A). Consistent with the selective advantage of WT lymphoid cells, we found high amounts of B and T cell reconstitution, measured as percentage (Fig. 1C) and absolute counts (Fig. 1D) at long-term follow-up after transplantation. Administration of 10% WT cells almost completely rescued the B and T cell lineages, and even administration of as little as 1% WT cells was still sufficient to support a partial reconstitution of both compartments and normalization of the CD4/CD8 ratio in the PB (Fig. 1E). A similar dose-dependent correction of B and T cell compartments and phenotypes was found at end-point analysis in the BM and spleen (fig. S3, B to E).

To determine what amount of correction is sufficient to confer in vivo resistance to viral infections, we challenged some of the transplanted mice with a high dose of lymphocytic choriomeningitis virus (LCMV). Mice reconstituted with increasing proportions of WT cells displayed a dose-dependent T cell response to the virus, measured both as increased total CD8$^+$ counts in PB and as a percentage of cells producing interferon-γ (IFN-γ) against an immunodominant viral peptide (Fig. 1F, left and middle panels). Whereas mice transplanted with 10% of WT HSPCs successfully cleared the virus, mice transplanted with 1% WT HSPCs developed fewer T cell clones responsive to LCMV

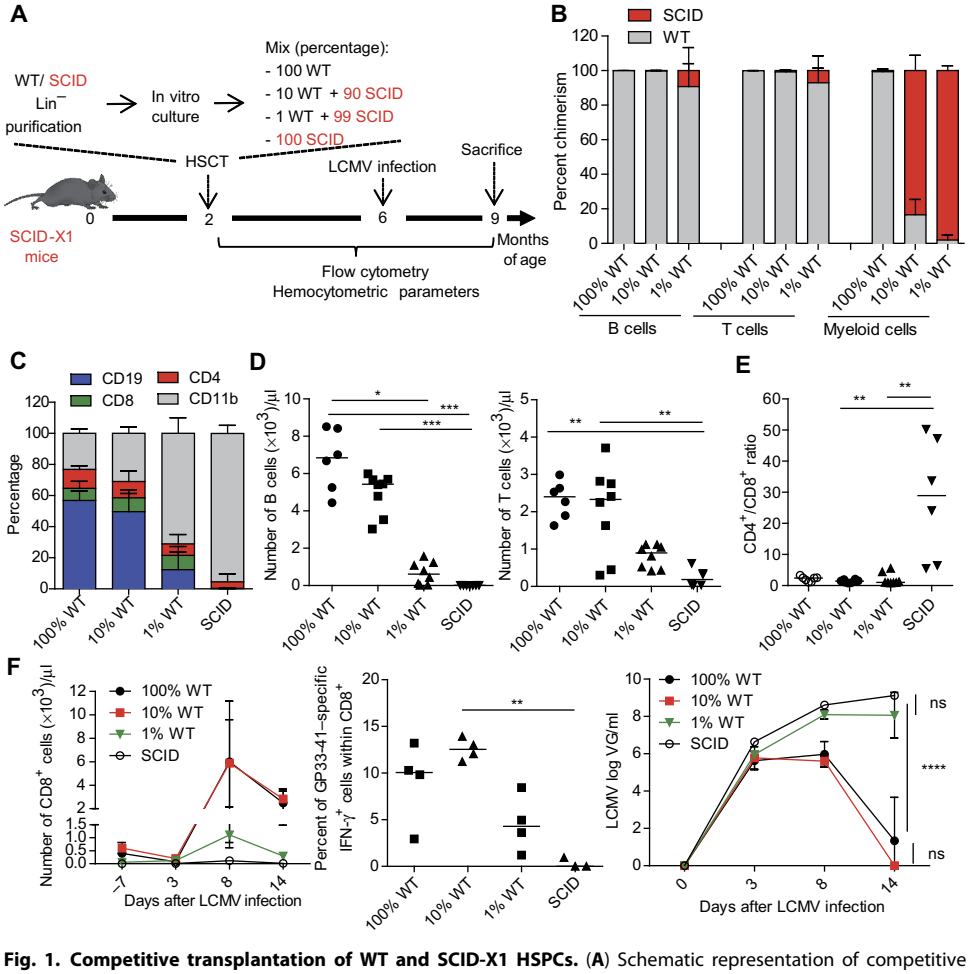

Fig. 1. Competitive transplantation of WT and SCID-X1 HSPCs. (**A**) Schematic representation of competitive transplant at different ratios of WT (black) and SCID-X1 Lin$^-$ HSPCs (red) into lethally irradiated SCID-X1 recipients. HSCT, hematopoietic stem cell transplantation. (**B**) Chimerism of WT and SCID-X1 cells observed within CD19$^+$ B cells, CD3$^+$ T cells, and CD11b$^+$ myeloid cells 15 weeks after transplant (n = 7 or 8 per group, pooled from two independent experiments). (**C**) Percent composition of myeloid and lymphoid lineages in PB 18 weeks after transplant. (**D**) Total counts of CD19$^+$ B cells (left) and CD3$^+$ T cells (right) in PB 18 weeks after transplant (Kruskal-Wallis test, median is plotted). (**E**) Ratio of CD4 to CD8 T cells in the PB of mice 12 weeks after transplant (Kruskal-Wallis test, median is plotted). (**F**) Left: Total number of CD8$^+$ T cells measured in PB at indicated times after LCMV Armstrong infection (100% WT, 10% WT, and 1% WT: n = 4; SCID: n = 3). Middle: Percent of CD8$^+$ cells producing IFN-γ measured in PB 8 days after LCMV infection (Kruskal-Wallis test, median is plotted). Right: LCMV titer [log viral genome (VG)/ml] measured in the serum [two-way analysis of variance (ANOVA)]. *P < 0.05, **P < 0.01, ***P < 0.001, and ****P < 0.0001. ns, not significant.

and achieved limited viral clearance (Fig. 1F, right panel). Overall, these results suggest that the threshold of functional HSPCs required to reconstitute immune function is between 1 and 10% of a standard transplant dose.

Safety and efficacy of reconstitution without conditioning

Because T cell reconstitution can be achieved in transplanted SCID-X1 patients even in the absence of conditioning regimens (*18*–*20*), we evaluated their impact on the reconstitution from a limited number of functional cells in competitive transplantation settings. By transplanting matched doses and ratios of WT to SCID-X1 HSPCs in SCID-X1 mice that were previously irradiated or not, we found that the transplanted progenitors colonized the thymus but did not engraft the primitive hematopoietic compartments of the BM in the absence of conditioning (fig. S4A), thus mainly providing T cell output (Fig. 2A). Mice transplanted without irradiation displayed a more robust T cell output from 3 to 6 weeks after HSPC administration, possibly as a result of better homing and expansion of progenitors within an undamaged thymic microenvironment (Fig. 2B) (*21*). When we measured the absolute T cell counts at long-term follow-up, we found less reconstitution without conditioning at all transplanted ratios (Fig. 2C), likely due to the limited naïve T cell output in the absence of a constant supply of progenitors from the BM (fig. S4B). Notably, 50% of the mice transplanted with WT cells without conditioning developed aggressive T cell lymphoblastic lymphomas starting from 20 weeks after infusion (Fig. 2D), unlike irradiated mice, which remained mostly tumor-free throughout the follow-up of the experiment. The tumors developed within the thymus, which became enlarged, and disseminated to other sites in some mice (Fig. 2, E and F, and fig. S4, C to G). Tumors originated from one or few clones, as determined by T cell receptor rearrangement analysis (fig. S5A), and possibly from committed T cell progenitors in the thymus, because similar malignancies were previously reported to develop from thymic grafts of normal mice in SCID recipients (*22*). The lymphomas were transplantable into immunodeficient and immunocompetent mice, in which they broadly infiltrated hematopoietic and nonhematopoietic organs (fig. S5B). Notably, upon stratifying the mice according to the input or engrafted fraction of transplanted WT HSPCs, we noticed that the fewer WT cells engrafted, the higher the fraction of mice (65%) that developed lymphomas (Fig. 2G). To unravel whether the protection from tumorigenesis observed upon conditioning is linked to the slower T cell reconstitution observed after TBI or the engraftment of HSPCs in the BM that maintain thymus colonization in the long term (*22*), we transplanted mice with a low WT HSPC input, shielding the thymus during irradiation (fig. S5C). After this procedure, T cell reconstitution showed a robust spike as in the nonirradiated mice but was then sustained at a higher level, likely because the mice established a pool of functional HSPCs in the BM (Fig. 2H and fig. S5D). These irradiated and shielded mice showed strongly reduced but not abrogated occurrence of thymic lymphoma compared to the nonirradiated mice, suggesting a partially protective effect from the engraftment of even a few corrected HSPCs within the BM in our SCID-X1 model (Fig. 2I).

Immune reconstitution with clinically relevant and new conditioning strategies

Because TBI is rarely used for transplant conditioning for nonmalignant diseases, we tested whether transplantation of 10% WT HSPCs would achieve full immune reconstitution with more clinically relevant regimens. Treatment of the mice with a myeloablative dose of

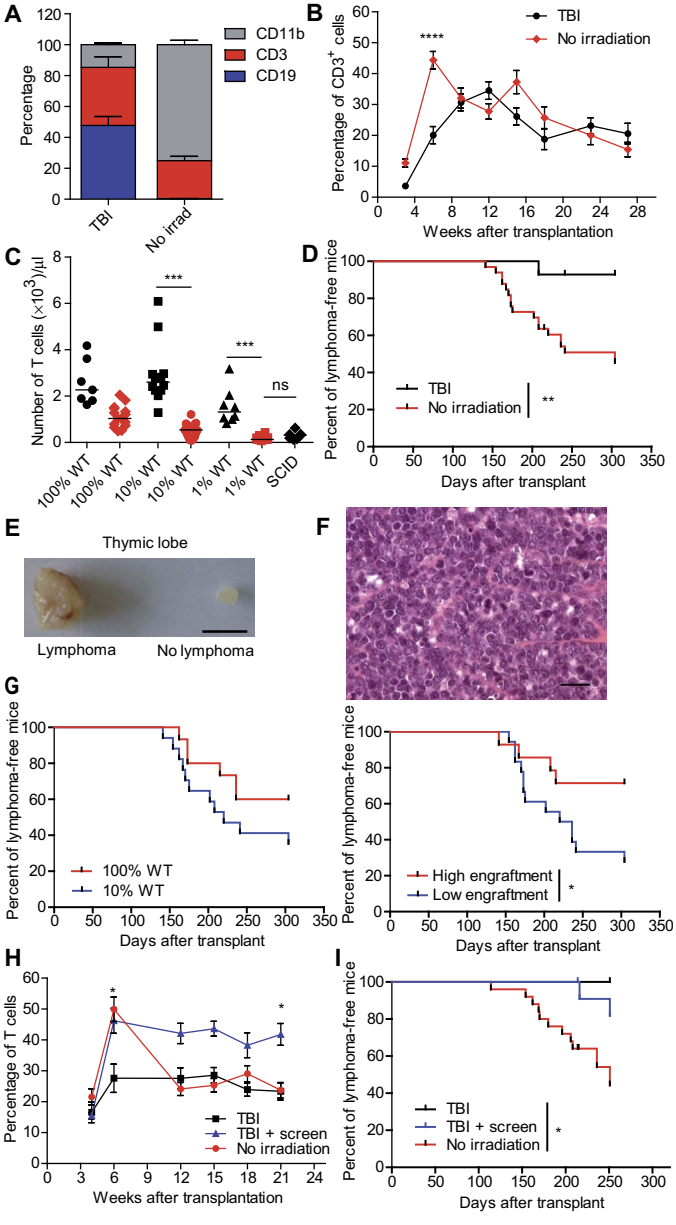

Fig. 2. Efficacy and safety of hematopoietic reconstitution without conditioning. (**A**) Percent composition of myeloid and lymphoid lineages in the PB 12 weeks after transplanting 10% WT cells without irradiation (No irrad; $n = 8$) or after lethal irradiation (TBI, $n = 10$) of recipient SCID-X1 mice. (**B**) Percentage of PB T cells at indicated times after transplant. TBI, $n = 15$; no irradiation, $n = 21$ (two-way ANOVA). (**C**) Total counts of PB T cells measured 12 weeks after transplant. 100% TBI groups (black), $n \geq 7$; no-irradiation groups (red), $n \geq 10$ (Kruskal-Wallis test, median is plotted). (**D**) Percentage of lymphoma-free animals in the follow-up of SCID-X1 mice transplanted with WT HSPCs with (TBI, $n = 14$) or without ($n = 32$) irradiation (log-rank test). (**E**) Representative image of a thymic lobe from a mouse with thymic lymphoma and a control C57BL/6 mouse. Scale bar, 1 cm. (**F**) Hematoxylin and eosin–stained section of thymic lymphoma. Scale bar, 20 μm. (**G**) Percentage of lymphoma-free mice as in (D) after stratifying the data according to the dose of WT cells transplanted without conditioning (100% WT, $n = 15$; 10% WT, $n = 17$) or the extent of PB engraftment with WT cells at 100 days after transplant (above or below 40% threshold). $P = 0.14$ and $P > 0.05$, respectively (log-rank test). (**H**) Percentage of T cells in PB of SCID-X1 mice transplanted with matched doses of WT cells without irradiation ($n = 25$) or after TBI without ($n = 8$) or with shielded thymus (TBI + screen, $n = 13$) (two-way ANOVA). (**I**) Percentage of lymphoma-free animals in transplanted SCID-X1 mice from (H) (*k*-sample log-rank test). *$P < 0.05$, **$P < 0.01$, ***$P < 0.001$, and ****$P < 0.0001$.

the alkylating agent treosulfan resulted in myeloid engraftment with WT cells approaching the input ratio, as observed after TBI, and full reconstitution of the lymphoid compartments (Fig. 3, A and B). We also explored a nongenotoxic strategy to selectively deplete hematopoietic cells with an immune toxin while sparing toxicity to the other organs, as recently reported (*23*). SCID-X1 mice were treated with a single dose of anti-CD45 antibodies conjugated to the protein synthesis inhibitor toxin saporin (CD45-SAP), which caused substantial depletion (~70%) of the HSPC compartments and milder depletion of the more mature cell populations (fig. S6, A to C), and transplanted with 10% WT cells 3 days later. Myeloid engraftment with WT cells was lower for CD45-SAP than for TBI, used as a reference, but stable in the follow-up, indicating successful HSC engraftment (Fig. 3C and fig. S6D). Notably, T cell reconstitution after CD45-SAP was faster and as robust as that achieved after TBI, despite the lower HSC engraftment, possibly because of the sparing of the thymus and BM environments, resulting in similar counts of circulating T cells at long-term follow-up (Fig. 3, D and E) and, upon LCMV challenge, similar expansion of total and virus-specific CD8 T cells and a considerable albeit less robust viral clearance (Fig. 3F). These findings confirm that an input of 10% functional HSPCs can support full lymphoid reconstitution across different conditioning strategies and highlight the potential advantages of a milder regimen that selectively targeted hematopoietic lineages and effectively rescued T lymphopoiesis even after engraftment of only a few percent of WT HSCs.

Functional validation of the edited human *IL2RG* gene in the SCID-X1 mouse model

To establish the therapeutic potential of a gene correction strategy for the treatment of SCID-X1, we developed protocols for gene editing in mouse HSPCs ("electro ZFN" and "lentiviral vector (LV) guide RNA (gRNA)"; fig. S7) targeting either intron 1 or exon 5 of *IL2RG* (fig. S7A). We first explored a procedure based on the delivery of donor DNA template by integrase-defective lentiviral vectors (IDLVs) and the transfection of *ZFN* mRNAs (fig. S7B, top). This protocol yielded high on-target nuclease activity and transgene integration (fig. S7C), but also high cytotoxicity, mostly due to the electroporation of exogenous mRNAs (fig. S7D). By sorting cells for Sca1 expression, we observed a lower proportion of edited cells—both by NHEJ and HDR—in the Sca1$^+$ fraction, which contains the more primitive HSPCs, suggesting lower activity of nucleases and/or more pronounced toxicity in this compartment (fig. S7E). After transplantation into SCID-X1 mice, we observed stable engraftment of green fluorescent protein–positive (GFP$^+$) cells in a fraction of mice (30%; fig. S7F), with marking confined to lymphoid cells, in which the corrected gene confers a selective growth advantage, and lack of engraftment of edited HSCs (fig. S7, G and H). To distinguish whether the lack of edited mouse HSCs might be due to hypersensitivity of these cells to mRNA electroporation or represents a general biological response of mouse HSPCs to DNA DSBs, as previously reported (*24*–*27*), or a specific liability of the SCID-X1 model, we used a transgenic mouse constitutively expressing SpCas9 (*28*). We verified robust Cas9 expression in the primitive hematopoietic compartments in both the homozygous and heterozygous mice (fig. S7I) and transiently expressed the gRNA in these cells by IDLV transduction (fig. S7J). We first targeted a locus expected to be neutral for hematopoiesis, the noncoding region of the *Ghr* gene, reaching up to 80% indels ex vivo with only mild toxicity (fig. S7K), and scored stable long-term maintenance of the edited cells upon transplantation in the mice, accounting for an average of 40% of the

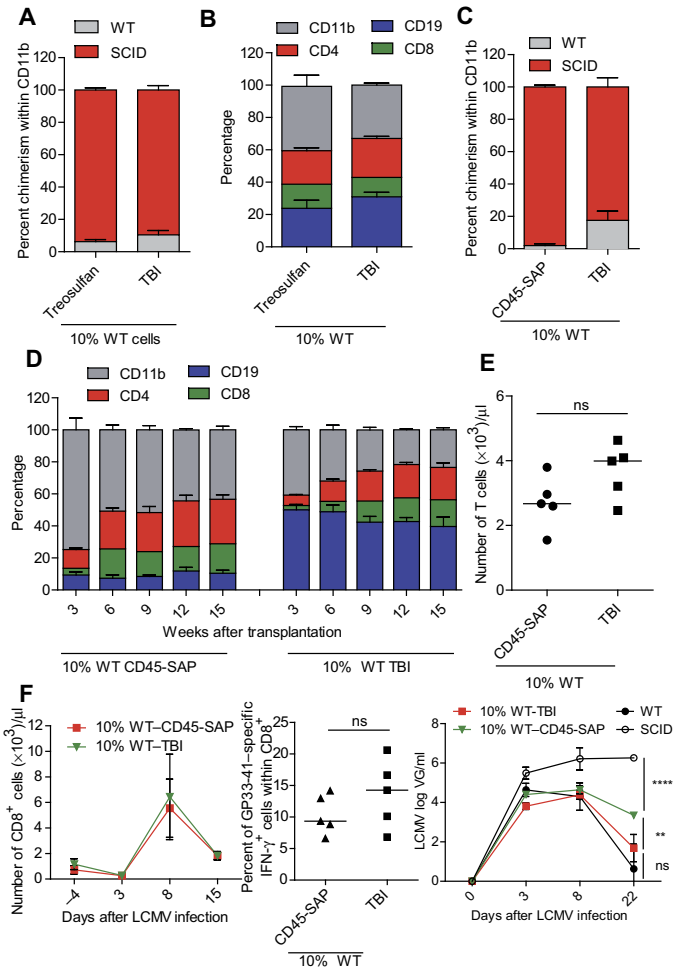

Fig. 3. Hematopoietic reconstitution with clinically relevant conditioning regimens. (**A**) Chimerism of WT and SCID-X1 cells observed within CD11b$^+$ myeloid cells 12 weeks after transplant of 10% WT Lin$^-$ cells after conditioning the recipients with TBI (n = 5) or treosulfan (n = 5). (**B**) Percent PB composition of myeloid and lymphoid lineages in mice from (A). (**C**) Chimerism of WT and SCID-X1 cells observed within CD11b$^+$ myeloid cells 15 weeks after transplant of 10% WT Lin$^-$ cells in recipients conditioned with TBI (n = 5) or CD45-SAP (n = 5). (**D**) Percent PB composition of myeloid and lymphoid lineages at the indicated times after transplant in mice from (C). (**E**) Total counts of CD3$^+$ T cells measured in PB 15 weeks after transplant in mice from (C) (Mann-Whitney test, median is plotted). (**F**) Left: Total number of CD8$^+$ T cells measured in PB at indicated times after LCMV Armstrong infection of mice from (C). Middle: Percent of CD8$^+$ cells producing IFN-γ measured in PB 8 days after LCMV infection (Mann-Whitney test, median is plotted). Right: LCMV titer (log VG/ml) measured in the serum at the indicated times; nontransplanted WT and SCID-X1 mice were used as controls. $^{**}P < 0.01$ and $^{***}P < 0.001$ (two-way ANOVA).

graft (fig. S7L). Upon sorting the different hematopoietic populations from the spleen and BM, we confirmed editing in lymphoid and myeloid lineages, as well as progenitors and HSCs from the BM (fig. S7M), demonstrating that the few DNA DSBs are well tolerated by mouse HSCs and do not impair their engraftment and long-term repopulation ability. To adapt the procedure to the correction of the SCID-X1 model, we crossed the Cas9 transgenic mice with SCID-X1 homozygous females and treated the male offspring (SCID-X1–Cas9$^{+/-}$ mice). SCID-X1–Cas9$^{+/-}$ HSPCs were transduced with an optimized protocol based on a single IDLV containing either of the two *IL2RG* donor

templates described above and expressing the cognate gRNA targeting a region within either ZFN cleavage site (fig. S7, N to P). By bypassing the nuclease mRNA delivery step, we alleviated the cytotoxicity of the ex vivo editing protocol in mouse HSCs (mean 93% live cells) and also obtained high levels of NHEJ and improved HDR within the Sca1$^+$ compartment (fig. S7, Q and R). By this procedure, we obtained engraftment of the edited cells in nearly all the transplanted SCID-X1 mice (93%; fig. S7S), with a median of 0.5% BM KLS$^+$ cells edited by HDR, as measured by the expression of the GFP marker knocked in with the corrective cDNA (fig. S7T) and substantial numbers of indels measured in *IL2RG* in circulating cells (fig. S7U). Overall, our data provide evidence of successful targeted gene editing of mouse lymphoid progenitors and HSCs, although it was still limited when the intended outcome was dependent on HDR.

By analyzing the cellular composition of the PB and spleen of the mice transplanted with SCID-X1 HSPCs treated for gene editing with these protocols, we observed the emergence of B cells and expanded and persistent T cells, unlike our findings in SCID-X1 mice transplanted with uncorrected HSPCs (Fig. 4A and fig. S8A). The mature lymphoid compartments were almost completely composed of GFP$^+$ cells, confirming the selective advantage of edited cells over the unedited SCID-X1 cells. The extent of T cell reconstitution achieved in these mice was similar to that obtained by transplanting 1% WT HSPCs (Fig. 4, B and C).

By characterizing the reconstituted lymphoid lineages within the BM and spleen, we found that the immunophenotype and distribution of the gene-corrected cells were similar to those of WT mice. In particular, the CD4/CD8 T cell ratio was completely restored (Fig. 4D). Moreover, whereas SCID-X1 B cell progenitors were blocked at the pre-pro-B early stage of differentiation, the corrected B cells normally progressed across all differentiation stages (Fig. 4E). Corrected B cells were also able to proliferate and up-regulate the CD69 activation marker when stimulated ex vivo (Fig. 4F). To test the functionality of the gene-corrected T cells, we harvested T cells from the spleen and confirmed their IL2RG-dependent proliferation in response to several stimuli with both exon 5 and intron 1 gene-correcting reagents (Fig. 4G and fig. S8B). Finally, we challenged the reconstituted mice with LCMV and observed emergence of viral-specific CD8$^+$ T cells expressing IFN-γ, demonstrating the ability of the corrected cells to engage in an effector response in vivo (Fig. 4H). Together, these results show that the transplantation of edited HSPCs can generate functional lymphoid progeny in the engrafted mice to an extent similar to that expected after transplanting a matched proportion of WT HSPCs, thus providing validation of our corrective gene knock-in strategy in a disease model. We did not detect occurrence of thymic lymphomagenesis in the follow-up of mice transplanted with edited HSPCs with either protocol, further supporting the protective role of conditioning when a small input of functional HSPCs is infused (fig. S8C).

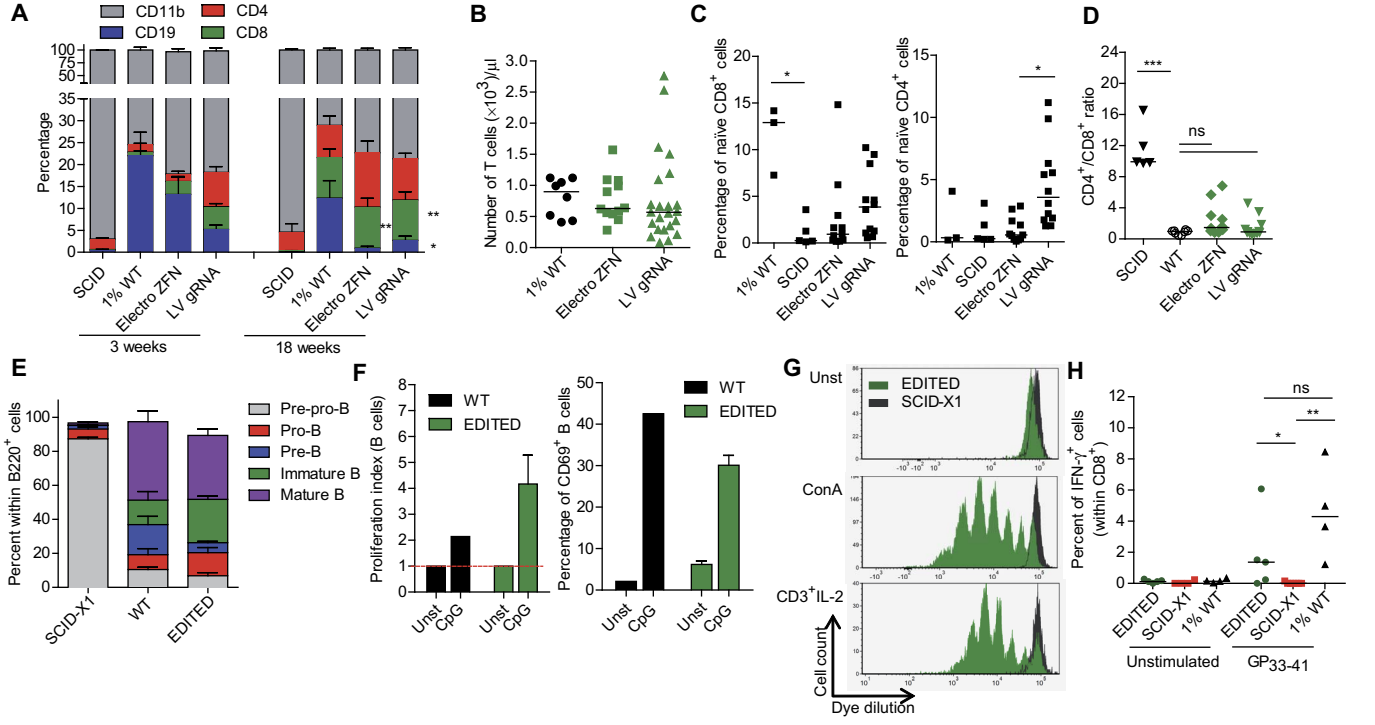

Fig. 4. Functional validation of *IL2RG*-edited lymphoid cells in transplanted mice. (**A**) Composition of myeloid and lymphoid lineages in PB after transplantation with SCID-X1 cells ($n = 7$), 1% WT cells ($n = 8$), or SCID-X1 cells treated with the exon 5 *IL2RG* electro ZFN ($n = 12$) or LV gRNA ($n = 15$) protocols. Significance is shown relative to SCID-X1. (**B**) PB T cell counts 18 weeks after transplant ($n = 8$, 12, and 20 for WT, electro ZFN, and LV gRNA, respectively). (**C**) Percentage of naïve cells within CD8$^+$ (left) and CD4$^+$ (right) splenic T cells ($n = 3$, 5, 11, and 12 for 1% WT, SCID, electro ZFN, and LV gRNA, respectively; median is plotted). (**D**) Ratio of CD4 to CD8 T cells in the spleen ≥21 weeks after transplant; untransplanted WT mice reported as controls ($n = 8$, median is plotted). (**E**) Percent of the indicated B cell subpopulations within BM B220$^+$ cells ≥21 weeks after transplant [SCID-X1, $n = 8$; WT, $n = 9$; EDITED (either of the protocols), $n = 15$]. (**F**) Proliferation index (left) and percentage of CD69$^+$ B cells (right) among exon 5 *IL2RG*-edited B cells from the spleen of transplanted mice ($n = 8$) or from a WT mouse as control, stimulated or not with unmethylated CpG oligodeoxynucleotides (CpG). Unst, unstimulated. (**G**) Cell proliferation measured by fluorescent dye dilution of exon 5 *IL2RG*-edited T cells and SCID-X1 cells, stimulated as indicated. ConA, concanavalin A. (**H**) Percentage of CD8$^+$ cells expressing IFN-γ from PB 7 days after LCMV infection of transplanted mice ($n = 5$, 7, and 4 for EDITED, SCID-X1, and 1% WT, respectively; Kruskal-Wallis test, median is plotted). *$P < 0.05$, **$P < 0.01$, and ***$P < 0.001$.

Efficient, highly specific, and scalable editing of human CD34$^+$ HSPCs for *IL2RG* gene correction

Having obtained functional evidence of the therapeutic potential of our gene correction strategy in the SCID-X1 mice, we aimed to optimize human HSPC gene editing to reach the threshold for safe reconstitution predicted in our SCID-X1 mouse model (≥10% *IL2RG* editing in the more primitive HSPC fraction). We focused on targeting the intron 1 *IL2RG* site to correct the vast majority of SCID-X1–causing mutations with the same reagents. Whereas the choice of donor template and the design of the edited locus could be stringently validated in our humanized mouse model, the same cannot be said of the specificity of the nucleases on the genome, given the species-specific sequence. For the studies described so far, we used a pair of six-finger ZFNs that was highly specific for the intended target, as gauged by the percentage of indels found by deep sequencing at the target site (66% indels at the highest ZFN dose) and all the off-target sites identified by an unbiased genome-wide screening (*29*). For the human HSPC studies, this pair was further optimized by mutations that reduce the affinity of the protein backbone for the phosphate group in the DNA and allow increased activity and selectivity of cleavage (Table 1 and table S2). The improved ZFNs gained >2 log in selectivity (ratio between on-target indels and the sum of indels at all interrogated off-target sites) over the pair used in the previous studies while displaying higher on-target activity and improved tolerability at increasing doses. To further validate the improved intron 1 *IL2RG* gene editing reagents on a human cell type that depends on expression of the targeted gene for survival and proliferation, we performed the editing procedure on primary T lymphocytes from male donors (which contain only one *IL2RG* allele). For comparison, we used ZFNs targeting exon 5 of *IL2RG* or an unrelated locus (*AAVS1*) (*30*). Whereas the subset of exon 5 *IL2RG*-edited cells that repaired the DNA DSBs by NHEJ, thus disrupting the reading frame of the gene, was counterselected shortly after the treatment, the subset of cells that repaired the break by HDR grew in culture similarly to the *AAVS1*-targeted control cells. Intron 1–targeted T cells that underwent NHEJ or HDR at the site, measured by a newly validated droplet digital polymerase chain reaction (ddPCR) assay (fig. S9A), expanded similarly to the other unedited or control cells, demonstrating that the intron 1–targeted cDNA supports survival and normal proliferation of human T cells (Fig. 5A and fig. S9, B to D). By evaluating the extent of γ-chain expression on the surface of the targeted cells, the closest amount of expression to that of nontargeted cells was obtained for a donor construct containing a codon usage optimized cDNA, likely compensating for the lack of multiple introns in the primary transcript of the edited gene (fig. S9E). The functionality of the edited allele was confirmed by showing similar kinetics and extent of phosphorylation of downstream effectors of the γ-chain signaling pathway between edited and unedited T cells upon cytokine stimulation (fig. S9F).

We then turned to CD34$^+$ HSPCs to establish a gene correction protocol that would be transferable to the clinic. We first investigated whether introducing exogenous RNA may trigger innate cellular responses potentially detrimental to cell fitness and found a substantial but transient up-regulation of several IFN-responsive genes (IRGs) in CD34$^+$ cells (fig. S10A). This response was specifically triggered by the exogenous RNA and amplified by the release of type I IFN in the culture medium, as shown by its blockade upon addition of the B18R IFN decoy receptor (fig. S10B). Because IFN exposure may be detrimental to HSC repopulation activity and may impair transduction by viral vectors carrying the donor template, we modified the *ZFN* mRNA during in vitro transcription by incorporation of base analogs that prevent recognition by cellular sensors. Furthermore, we purified the mRNAs by high-performance liquid chromatography (HPLC) to remove shorter RNA contaminants. Both strategies strongly reduced IRG up-regulation, and their combination nearly completely abrogated this IRG response (fig. S10C) and increased HDR-mediated editing in all HSPC subpopulations, including the most primitive fraction (fig. S10D). We then treated CD34$^+$ cells derived from the cord blood (CB) of a SCID-X1 patient (bearing the R289X mutation) and showed extensive editing of the targeted locus (Fig. 5B).

To further optimize editing, we evaluated whether using an adeno-associated virus type 6 (AAV6) donor DNA vehicle shortly after mRNA electroporation could yield higher rates of gene editing, as recently reported (*9*, *10*), and achieved up to fivefold higher HDR-mediated gene editing over IDLV-treated cells in all hematopoietic subpopulations analyzed (mean 27% in the most primitive CD34$^+$ CD133$^+$ CD90$^+$ cells). This increase was observed for both CB- and BM-derived CD34$^+$ cells (Fig. 5C and fig. S10, E and F). Similar editing efficiencies were also obtained by using state-of-the-art CRISPR/Cas9 reagents targeting the same locus and delivered as ribonucleoprotein complexes (*10*), demonstrating the portability of our procedure to other editing platforms, although we did not further investigate the latter in this study (Fig. 5C). We did not observe any significant changes in the relative composition of the hematopoietic subpopulations 3 days after the treatment compared to untreated controls, suggesting that the optimized gene editing procedure did not adversely affect the survival and growth of the more primitive cells (Fig. 5D and fig. S10F, right panel). By transplanting the ZFN + IDLV or AAV6-treated cells into nonobese diabetic SCID γ (NSG) mice, we obtained comparably high long-term human cell engraftment (Fig. 5E) but with a significantly higher fraction of HDR-edited cells in the AAV6 treatment group ($P < 0.05$), reaching an average of 13% in the PB (Fig. 5F) and >20% in the sorted myeloid,

Table 1. Off-target quantification for optimized intron 1 *IL2RG* ZFNs. Percentages of indels measured by deep sequencing at the on-target and three off-target sites, as well as cell viability for mobilized human PB CD34$^+$ cells treated with the selected intron 1 *IL2RG* ZFN lead pair or its optimized version. *$P < 0.01$ (Bonferroni significance). OT, off-target site.

ZFN	Dose (μg/ml)	On	OT1	OT4	OT6	On/ΣOT	% Cell viability
57629 + 57718	20	64.69*	6.18*	0.03	0.08	10.27	76.35
	40	65.78*	14.88*	0.09*	0.45*	4.27	67.85
57629 improved version + 57718 improved version	20	74.53*	0.05	0.04	0.02	710.46	74.40
	40	79.71*	0.03	0.03	0.05	733.99	74.75

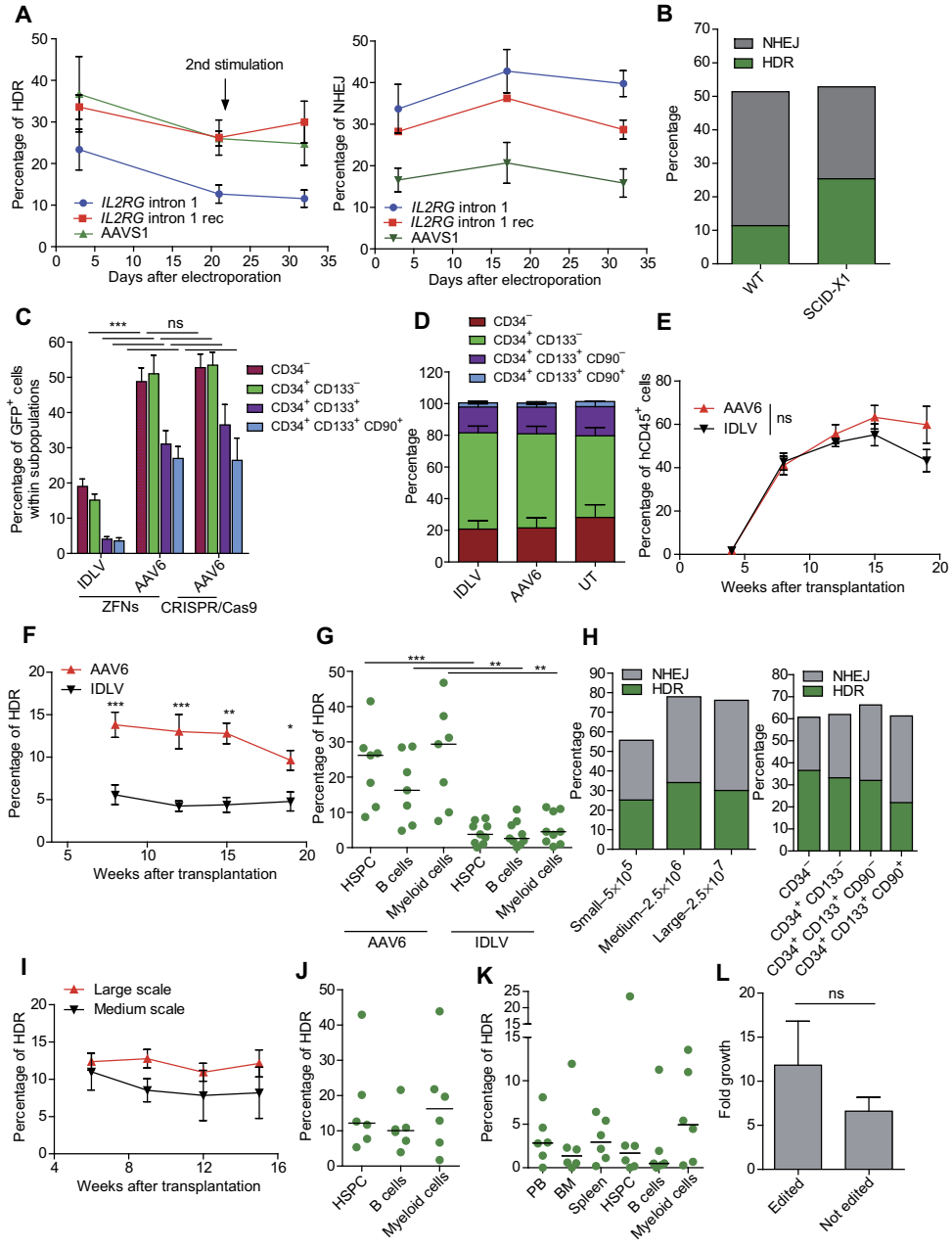

Fig. 5. Efficient and scalable *IL2RG* editing in human CD34$^+$ and T cells. (**A**) Percentage of primary human male T cells edited by HDR (left) or NHEJ (right) at intron 1 *IL2RG* using WT (intron 1 *IL2RG*, $n = 6$) or codon usage optimized (intron 1 *IL2RG* rec, $n = 9$) donor template or edited at *AAVS1* ($n = 3$). (**B**) HDR and NHEJ 3 days after intron 1 *IL2RG* gene editing of CB CD34$^+$ cells from an SCID-X1 patient (R289X) or WT cells as control. (**C**) Percentage of GFP$^+$ cells measured within the indicated subpopulations 3 days after intron 1 *IL2RG* editing of CB-derived CD34$^+$ using the indicated donor template vector and nuclease ($n = 5$, 7, and 6 for IDLV + ZFN, AAV6 + ZFN, and AAV6 + CRISPR/Cas9, respectively; Mann-Whitney test). (**D**) Subpopulation composition of treated CD34$^+$ cells from (C). (**E**) Human CD45$^+$ cell engraftment in PB at indicated times after transplantation of CB CD34$^+$ cells edited at intron 1 *IL2RG* using IDLV ($n = 7$) or AAV6 as donor ($n = 9$) (two-way ANOVA). (**F**) Percentage of HDR within human cells measured by ddPCR in mice from (E) ($n = 9$; two-way ANOVA). (**G**) Percentage of HDR measured by ddPCR in sorted BM CD34$^+$ HSPCs, CD19$^+$ B cells, and CD33$^+$ myeloid cells from mice in (E) (Mann-Whitney test, median is plotted). (**H**) HDR and NHEJ 3 days after intron 1 *IL2RG* editing of increasing amounts of CB-derived CD34$^+$ cells in bulk population (left) or within sorted subpopulations (right). (**I**) Percentage of HDR editing within human cells from mice transplanted with medium-scale ($n = 6$) or large-scale ($n = 12$) *IL2RG*-edited CD34$^+$ cells from (H). (**J**) Percentage of HDR as in (G) from large-scale transplanted mice at the 23-week end point ($n = 6$; median is plotted). (**K**) Percentage of HDR measured in the indicated organs and sorted cells as in (G) 12 weeks upon secondary transplant of human CD34$^+$ cells from mice in (I) ($n = 6$, median is plotted). (**L**) Ex vivo growth of *IL2RG*-edited and unedited T cells ($n = 9$) from the spleen of NSG mice transplanted with edited CD34$^+$ cells upon stimulation with γ-chain–dependent cytokines (Mann-Whitney test). *$P < 0.05$, **$P < 0.01$, ***$P < 0.001$.

lymphoid, and progenitor cell populations from the BM (Fig. 5G), consistent with the higher rates of HDR measured in the most primitive cell fraction in the ex vivo culture.

To mimic a clinically ready protocol for HSPC gene editing, we scaled up the entire process using a donor template lacking the GFP reporter cassette. We treated up to 2.5×10^7 CB-derived CD34$^+$ cells with the optimized reagents and reproduced the high rates of editing observed at small scale within the different hematopoietic subpopulations, analyzed after cell sorting (Fig. 5H). Deep sequencing performed on the treated CD34$^+$ cells confirmed the high specificity of the optimized ZFNs. We did not detect significant amounts of modification above the threshold of sensitivity in any of the off-target sites identified by unbiased genome-wide screening for the earlier generation ZFN set in the bulk or sorted subpopulations (Table 2). Transplantation of large-scale treated cells into NSG mice confirmed robust engraftment and HDR-mediated editing, which was also detected upon serial transplantation in secondary recipients (Fig. 5, I to K, and fig. S10G). *IL2RG*-edited T cells harvested from transplanted mice grew ex vivo in the presence of γ-chain–dependent cytokines to a similar extent as their unedited counterparts, further confirming their functionality (Fig. 5L). Overall, these results indicate that we can reach the threshold of *IL2RG* gene editing for safe and efficient correction of SCID-X1 established in our preclinical model in human long-term repopulating HSPCs.

DISCUSSION

Here, we report preclinical studies geared toward clinical translation of targeted genome editing of HSCs and its application to the stable correction of SCID-X1 disease. The proportion of functional HSPCs in the cell product required to correct the disease in our mouse model (~10%) was determined using cells expressing the WT murine *Il2rg*. This figure was true across different types of conditioning, including TBI, myeloablative chemotherapy, and a milder immunotoxin-based selective depletion of hematopoietic cells. Whereas the two myeloablative strategies (TBI

Table 2. On- and off-target analysis in CD34$^+$ cells treated at increasing scales for intron 1 *IL2RG* editing with optimized ZFNs. Percentages of indels at the ZFN on-target and identified off-target sites measured by deep sequencing from samples shown in Fig. 5H. LS, large-scale treated CD34$^+$ cells; MS, medium-scale treated CD34$^+$ cells; SS, small-scale treated CD34$^+$ cells. *P < 0.01 (Bonferroni significance) compared to untreated sample (UT).

Sample	On	OT1	OT2	OT3	OT4	OT5	OT6	OT7
LS bulk	40.84*	0.05	0.10	0.18	0.04	0.04	0.04	0.03
MS bulk	66.48*	0.03	0.08	0.18	0.03	0.03	0.04	0.01
SS bulk	65.87*	0.05	0.12	0.14	0.04	0.06	0.03	0.02
LS CD34$^-$	38.09*	0.07	0.08	0.16	0.02	0.02	0.03	0.03
LS CD34$^+$ CD133$^-$	43.03*	0.06	0.13	0.17	0.03	0.03	0.04	0.03
LS CD34$^+$ CD133$^+$ CD90$^-$	50.41*	0.11	0.11	0.13	0.04	0.04	0.05	0.04
LS CD34$^+$ CD133$^+$ CD90$^+$	50.40*	0.10	0.10	0.14	0.03	0.03	0.02	0.05
UT	0.03	0.05	0.11	0.13	0.02	0.02	0.03	0.04

and chemotherapy) established a WT HSC chimerism in the BM reflecting the input ratio, the biological conditioning was less efficient but still resulted in robust lymphoid reconstitution, likely because of better preservation of the tissue niches. This finding is encouraging from the perspective of clinical translation, because treatment of SCID-X1 would most likely rely on a mild conditioning regimen that may lower the proportion of engrafted HSCs from the administered cell product. Extrapolation of the mouse data to the human setting should also consider the following aspects. Whereas the thymus in SCID-X1 mice is hypomorphic but its overall structure is partially preserved, this organ is more severely affected by the disease in humans, possibly hindering the extent of reconstitution, even if the T cell compartment is successfully restored upon allogeneic transplantation or autologous gene therapy. On the other hand, the complete lack of T cells in SCID-X1 children might provide for lower competition in the thymus than observed in SCID-X1 mice, thus resulting in overestimation of the threshold in the mouse model. Overall, our prediction that engraftment of ≥10% corrected HSPCs will provide benefits in human patients is in line with recent clinical data on LV-based gene therapy for SCID-X1, where patients showing a vector copy number ≤0.1 in the HSC and myeloid compartments showed substantial clinical improvement (*31*).

TBI before transplant also protected the mice from an unexpectedly high incidence of thymic lymphoma during long-term follow-up. Our findings suggest that these tumors might arise as a consequence of sustained thymocyte proliferation from a limited input of administered progenitors that lack or have limited replenishment from the BM and a preserved thymic microenvironment allowing their rapid growth. The increasing rate of tumorigenesis in mice receiving a lower input of functional cells suggests that the fewer *Il2rg*$^{+/+}$ thymic progenitors contribute to thymopoiesis, the stronger the replicative stress they are subjected to, raising concerns for the long-term safety of functional reconstitution by a limiting number of corrected progenitors. Our findings are consistent with a previous report of tumorigenesis from WT thymic progenitors growing in the absence of BM replacement in SCID mice (*22*) and further supported by a recent study in another model of SCID-X1, where thymic lymphomas arose upon limiting transplant doses after sublethal irradiation as conditioning (*32*). Although the lymphomagenesis observed in transplanted SCID-X1 mice might be a mouse-specific effect, it could help in explaining the high leukemia incidence observed in SCID-X1 gene therapy trials performed with early-generation vectors (*33*), at variance with gene therapy trials performed for adenosine deaminase–SCID with a similar type of vector but including administration of a mild conditioning regimen to allow some HSC engraftment. The inverse dependence of lymphomagenesis on input cell dose might help explain why no leukemic events have been reported in SCID patients after allogeneic BM transplantation, which is usually performed without conditioning but with the infusion of a full dose of functional donor cells (*20*).

We demonstrated functional correction of the edited human gene in vivo by developing a gene editing protocol for mouse HSPCs. Whereas previous reports showed strong impairment of self-renewal and repopulation ability of mouse HSPCs with multiple DNA DSBs (*24*–*27*), we showed that a few nuclease-induced DNA DSBs are well tolerated by primitive KLS cells. However, mouse HSCs were exceedingly sensitive to electroporation (see fig. S7D), which we had to bypass, using viral transduction and/or transgenesis to achieve robust expression of the editing machinery without excess toxicity. Using these protocols, we achieved high and stable rates of NHEJ-mediated gene editing in the reconstituted hematopoiesis, which should be useful for future gene discovery and functional studies on mouse HSCs. However, HDR-mediated gene editing was much lower, although still detectable long-term after transplant and sufficient for providing functional readouts of the edited HSC output.

A potential limitation of testing the functionality of human genes in the mouse cell context is the failure to fully reconstitute protein-protein interactions across species, which may result in underestimation of efficacy. Here, however, HSPCs with edited human *IL2RG* rescued the investigated SCID-X1 phenotypes with similar efficiency as WT mouse cells, thus indicating functional cross-reaction of the human γ subunit with the other murine subunits contributing to cytokines binding in the receptor complexes. These data agree with previous reports of functional reconstitution of mouse lymphoid compartments after human *IL2RG* gene transfer using γ-retroviral and lentiviral vectors (*34*, *35*).

Notably, HDR-mediated editing was substantially higher in human than mouse HSPCs, possibly because of the improved quality and specificity attained for the editing reagents and the optimization of the culture conditions for human HSPCs, which better support their ex vivo proliferation while reducing the impact on their repopulation capacity. The enhancement of HDR-mediated editing in SCID-repopulating cells using AAV6 in our study is substantial even with respect to the studies that first reported the advantage of using this donor DNA vehicle in HSPC editing (*9*, *10*). This improved benefit might be due to the suppression of type I IFN release after the electroporation procedure, which likely impairs subsequent transduction by viral vectors. Notably, conversion of a single base-pair mutation to the normal sequence with similarly high efficiency to that shown here was recently reported in SCID-repopulating human HSPCs using an oligonucleotide donor, although this outcome required individualized editing reagents and optimized correction protocols (*11*). Our protocol was reproducible across several donors and HSPC sources, portable to the CRISPR/Cas9 platform, scalable to large numbers of treated HSPCs, and achieved yields of edited SCID-repopulating HSPCs, meeting the predicted threshold for safe immune reconstitution according to our mouse model studies.

Our study supports a rationale for moving toward clinical testing of HSPC gene correction in SCID-X1 patients who lack a compatible HSC

donor and would be at high risk if undergoing allogeneic hematopoietic stem cell transplantation (HSCT). Administration of the autologous edited HSPCs could be performed upon partial conditioning, aiming to establish sufficient engraftment of corrected HSCs to provide long-lasting reconstitution of T cell, B cell, and natural killer cell lineages (*31*). An alternative treatment for these patients is conventional gene replacement using self inactivating-γ-retroviral vectors or LVs, which have been investigated in recent clinical trials (*19*, *31*). Whereas extensive clinical data show safe, robust, and stable engraftment of LV-modified HSCs in several disease settings (*36*), the specific features of SCID-X1 discussed above may exacerbate any residual risk of insertional mutagenesis and constitutive transgene expression, supporting the potential benefits of a more precise gene correction strategy. On the other hand, there are still several unknowns concerning initial clinical testing of HDR-mediated HSPC editing that may be difficult to comprehensively address in preclinical models, including the genotoxic risk associated with any residual off-target activity of the nucleases and the impact of DNA DSBs on the long-term repopulation capacity of HSCs in humans. Ultimately, a stringent risk/benefit assessment of either gene therapy strategy will only come from clinical testing and the long-term follow-up of treated patients. Whether they will be applied to SCID-X1 or other diseases with even stronger requirements for faithful reconstitution of the affected gene, our results pave the way toward clinical translation of targeted HSC gene editing by drafting a roadmap of preclinical studies to interrogate the efficacy and safety of the procedure and establishing clinically compatible processes for efficient manufacturing of the therapeutic cell product.

MATERIALS AND METHODS

Study design

The objectives of this study were to establish the conditions for safe and effective correction of SCID-X1 in a humanized mouse model of the disease, used here as representative of functionally γ-chain–negative mice, and to validate a gene correction strategy for *IL2RG* in HSPCs. Kinetics and extent of hematopoietic reconstitution from limited input of WT or gene-edited HSPCs were analyzed in transplanted SCID-X1 mice upon different types of conditioning. Functionality of *IL2RG*-edited cells was verified using in vivo and in vitro functional studies. Optimization of treatment protocols and gene editing reagents was performed on mouse and human HSPCs to determine their effects on gene editing efficiency and in vivo repopulation capacity. Mice were randomized to treatment groups, without blinding. Criteria applied for mouse termination before the established end point were in accordance with the Institutional Animal Care and Use Committee protocol of the San Raffaele Scientific Institute. Cohort sizes were informed by previous experiments and by the total number of available treated cells; no outliers were excluded.

Statistical analyses

When normality assumptions were not met, nonparametric statistical tests were performed. Mann-Whitney test or Kruskal-Wallis test with Dunn's multiple comparison post hoc test were performed when comparing two or more groups, respectively. For paired observations, Wilcoxon matched-pairs signed-rank test was performed. For repeated measures over time, two-way ANOVA with Bonferroni's multiple comparison post-test was used. For survival studies, log-rank (Mantel-Cox) test was used for pairwise comparison, and *k*-sample log-rank test was used when comparing three groups. Values are expressed as means ± SEM unless otherwise indicated. Percentage values were transformed into a log-odds scale to perform parametric statistical analyses.

SUPPLEMENTARY MATERIALS

www.sciencetranslationalmedicine.org/cgi/content/full/9/411/eaan0820/DC1

Materials and Methods

Fig. S1. Humanized SCID-X1 mice.

Fig. S2. Phenotypical and functional characterization of humanized SCID-X1 mice.

Fig. S3. Hematopoietic reconstitution and functional studies of WT/SCID-X1 competitive transplants.

Fig. S4. Phenotypical characterization of lymphoblastic T lymphomas developing in mice transplanted without irradiation.

Fig. S5. Molecular and functional characterization of T lymphoma.

Fig. S6. Depletion of hematopoietic compartments with CD45-SAP in SCID-X1 mice.

Fig. S7. Development of a gene editing strategy for mouse HSPCs.

Fig. S8. Functionality of gene-edited lymphoid cells from transplanted mice.

Fig. S9. Functional validation of *IL2RG*-edited primary human T cells.

Fig. S10. Tailoring of gene editing protocol for human HSPCs.

Table S1. Phenotypical characterization of humanized SCID-X1 mice.

Table S2. Intron 1 *IL2RG* ZFNs off-target list.

Table S3. List of genomic gRNA target sequences.

Table S4. List of primers and probes.

Table S5. List of antibodies for flow cytometry.

Table S6. Raw data for Table 2 (provided as an Excel file).

References (*37*–*43*)

REFERENCES AND NOTES

1. J. A. Doudna, E. Charpentier, The new frontier of genome engineering with CRISPR-Cas9. *Science* **346**, 1258096 (2014).
2. H. Kim, J.-S. Kim, A guide to genome engineering with programmable nucleases. *Nat. Rev. Genet.* **15**, 321–334 (2014).
3. A. Lombardo, P. Genovese, C. M. Beausejour, S. Colleoni, Y.-L. Lee, K. A. Kim, D. Ando, F. D. Urnov, C. Galli, P. D. Gregory, M. C. Holmes, L. Naldini, Gene editing in human stem cells using zinc finger nucleases and integrase-defective lentiviral vector delivery. *Nat. Biotechnol.* **25**, 1298–1306 (2007).
4. H. Li, V. Haurigot, Y. Doyon, T. Li, S. Y. Wong, A. S. Bhagwat, N. Malani, X. M. Anguela, R. Sharma, L. Ivanciu, S. L. Murphy, J. D. Finn, F. R. Khazi, S. Zhou, D. E. Paschon, E. J. Rebar, F. D. Bushman, P. D. Gregory, M. C. Holmes, K. A. High, In vivo genome editing restores haemostasis in a mouse model of haemophilia. *Nature* **475**, 217–221 (2011).
5. A. Barzel, N. K. Paulk, Y. Shi, Y. Huang, K. Chu, F. Zhang, P. N. Valdmanis, L. P. Spector, M. H. Porteus, K. M. Gaensler, M. A. Kay, Promoterless gene targeting without nucleases ameliorates haemophilia B in mice. *Nature* **517**, 360–364 (2015).
6. N. Hubbard, D. Hagin, K. Sommer, Y. Song, I. Khan, C. Clough, H. D. Ochs, D. J. Rawlings, A. M. Scharenberg, T. R. Torgerson, Targeted gene editing restores regulated CD40L function in X-linked hyper-IgM syndrome. *Blood* **127**, 2513–2522 (2016).
7. P. Genovese, G. Schiroli, G. Escobar, T. Di Tomaso, C. Firrito, A. Calabria, D. Moi, R. Mazzieri, C. Bonini, M. C. Holmes, P. D. Gregory, M. van der Burg, B. Gentner, E. Montini, A. Lombardo, L. Naldini, Targeted genome editing in human repopulating haematopoietic stem cells. *Nature* **510**, 235–240 (2014).
8. J. Wang, C. M. Exline, J. J. DeClercq, G. N. Llewellyn, S. B. Hayward, P. W.-L. Li, D. A. Shivak, R. T. Surosky, P. D. Gregory, M. C. Holmes, P. M. Cannon, Homology-driven genome editing in hematopoietic stem and progenitor cells using ZFN mRNA and AAV6 donors. *Nat. Biotechnol.* **33**, 1256–1263 (2015).
9. S. S. De Ravin, A. Reik, P.-Q. Liu, L. Li, X. Wu, L. Su, C. Raley, N. Theobald, U. Choi, A. H. Song, A. Chan, J. R. Pearl, D. E. Paschon, J. Lee, H. Newcombe, S. Koontz, C. Sweeney, D. A. Shivak, K. A. Zarember, M. V. Peshwa, P. D. Gregory, F. D. Urnov, H. L. Malech, Targeted gene addition in human $CD34^+$ hematopoietic cells for correction of X-linked chronic granulomatous disease. *Nat. Biotechnol.* **34**, 424–429 (2016).
10. D. P. Dever, R. O. Bak, A. Reinisch, J. Camarena, G. Washington, C. E. Nicolas, M. Pavel-Dinu, N. Saxena, A. B. Wilkens, S. Mantri, N. Uchida, A. Hendel, A. Narla, R. Majeti, K. I. Weinberg, M. H. Porteus, CRISPR/Cas9 β-globin gene targeting in human haematopoietic stem cells. *Nature* **539**, 384–389 (2016).
11. S. S. De Ravin, L. Li, X. Wu, U. Choi, C. Allen, S. Koontz, J. Lee, N. Theobald-Whiting, J. Chu, M. Garofalo, C. Sweeney, L. Kardava, S. Moir, A. Viley, P. Natarajan, L. Su, D. Kuhns, K. A. Zarember, M. V. Peshwa, H. L. Malech, CRISPR-Cas9 gene repair of hematopoietic stem cells from patients with X-linked chronic granulomatous disease. *Sci. Transl. Med.* **9**, eaah3480 (2017).
12. C. W. Peterson, J. Wang, K. K. Norman, Z. K. Norgaard, O. Humbert, C. K. Tse, J. J. Yan, R. G. Trimble, D. A. Shivak, E. J. Rebar, P. D. Gregory, M. C. Holmes, H.-P. Kiem, Long-term

multilineage engraftment of autologous genome-edited hematopoietic stem cells in nonhuman primates. *Blood* **127**, 2416–2426 (2016).
13. J. M. Puck, A. E. Pepper, P. S. Henthorn, F. Candotti, J. Isakov, T. Whitwam, M. E. Conley, R. E. Fischer, H. M. Rosenblatt, T. N. Small, R. H. Buckley, Mutation analysis of IL2RG in human X-linked severe combined immunodeficiency. *Blood* **89**, 1968–1977 (1997).
14. X. Cao, E. W. Shores, J. Hu-Li, M. R. Anver, B. L. Kelsall, S. M. Russell, J. Drago, M. Noguchi, A. Grinberg, E. T. Bloom, W. E. Paul, S. I. Katz, P. E. Love, W. J. Leonard, Defective lymphoid development in mice lacking expression of the common cytokine receptor gamma chain. *Immunity* **2**, 223–238 (1995).
15. J. P. DiSanto, W. Müller, D. Guy-Grand, A. Fischer, K. Rajewsky, Lymphoid development in mice with a targeted deletion of the interleukin 2 receptor gamma chain. *Proc. Natl. Acad. Sci. U.S.A.* **92**, 377–381 (1995).
16. K. Ohbo, T. Suda, M. Hashiyama, A. Mantani, M. Ikebe, K. Miyakawa, M. Moriyama, M. Nakamura, M. Katsuki, K. Takahashi, K. Yamamura, K. Sugamura, Modulation of hematopoiesis in mice with a truncated mutant of the interleukin-2 receptor gamma chain. *Blood* **87**, 956–967 (1996).
17. R. Kumar, V. Fossati, M. Israel, H.-W. Snoeck, Lin$^-$Sca1$^+$Kit$^-$ bone marrow cells contain early lymphoid-committed precursors that are distinct from common lymphoid progenitors. *J. Immunol.* **181**, 7507–7513 (2008).
18. S. Hacein-Bey-Abina, F. Le Deist, F. Carlier, C. Bouneaud, C. Hue, J.-P. De Villartay, A. J. Thrasher, N. Wulffraat, R. Sorensen, S. Dupuis-Girod, A. Fischer, E. G. Davies, W. Kuis, L. Leiva, M. Cavazzana-Calvo, Sustained correction of X-linked severe combined immunodeficiency by ex vivo gene therapy. *N. Engl. J. Med.* **346**, 1185–1193 (2002).
19. S. Hacein-Bey-Abina, S.-Y. Pai, H. B. Gaspar, M. Armant, C. C. Berry, S. Blanche, J. Bleesing, J. Blondeau, H. de Boer, K. F. Buckland, L. Caccavelli, G. Cros, S. De Oliveira, K. S. Fernández, D. Guo, C. E. Harris, G. Hopkins, L. E. Lehmann, A. Lim, W. B. London, J. C. M. van der Loo, N. Malani, F. Male, P. Malik, M. A. Marinovic, A.-M. McNicol, D. Moshous, B. Neven, M. Oleastro, C. Picard, J. Ritz, C. Rivat, A. Schambach, K. L. Shaw, E. A. Sherman, L. E. Silberstein, E. Six, F. Touzot, A. Tsytsykova, J. Xu-Bayford, C. Baum, F. D. Bushman, A. Fischer, D. B. Kohn, A. H. Filipovich, L. D. Notarangelo, M. Cavazzana, D. A. Williams, A. J. Thrasher, A modified γ-retrovirus vector for X-linked severe combined immunodeficiency. *N. Engl. J. Med.* **371**, 1407–1417 (2014).
20. S.-Y. Pai, B. R. Logan, L. M. Griffith, R. H. Buckley, R. E. Parrott, C. C. Dvorak, N. Kapoor, I. C. Hanson, A. H. Filipovich, S. Jyonouchi, K. E. Sullivan, T. N. Small, L. Burroughs, S. Skoda-Smith, A. E. Haight, A. Grizzle, M. A. Pulsipher, K. W. Chan, R. L. Fuleihan, E. Haddad, B. Loechelt, V. M. Aquino, A. Gillio, J. Davis, A. Knutsen, A. R. Smith, T. B. Moore, M. L. Schroeder, F. D. Goldman, J. A. Connelly, M. H. Porteus, Q. Xiang, W. T. Shearer, T. A. Fleisher, D. B. Kohn, J. M. Puck, L. D. Notarangelo, M. J. Cowan, R. J. O'Reilly, Transplantation outcomes for severe combined immunodeficiency, 2000–2009. *N. Engl. J. Med.* **371**, 434–446 (2014).
21. S. L. Zhang, X. Wang, S. Manna, D. A. Zlotoff, J. L. Bryson, B. R. Blazar, A. Bhandoola, Chemokine treatment rescues profound T-lineage progenitor homing defect after bone marrow transplant conditioning in mice. *Blood* **124**, 296–304 (2014).
22. V. C. Martins, K. Busch, D. Juraeva, C. Blum, C. Ludwig, V. Rasche, F. Lasitschka, S. E. Mastitsky, B. Brors, T. Hielscher, H. J. Fehling, H.-R. Rodewald, Cell competition is a tumour suppressor mechanism in the thymus. *Nature* **509**, 465–470 (2014).
23. R. Palchaudhuri, B. Saez, J. Hoggatt, A. Schajnovitz, D. B. Sykes, T. A. Tate, A. Czechowicz, Y. Kfoury, F. Ruchika, D. J. Rossi, G. L. Verdine, M. K. Mansour, D. T. Scadden, Non-genotoxic conditioning for hematopoietic stem cell transplantation using a hematopoietic-cell-specific internalizing immunotoxin. *Nat. Biotechnol.* **34**, 738–745 (2016).
24. J. Wang, Q. Sun, Y. Morita, H. Jiang, A. Groβ, A. Lechel, K. Hildner, L. M. Guachalla, A. Gompf, D. Hartmann, A. Schambach, T. Wuestefeld, D. Dauch, H. Schrezenmeier, W.-K. Hofmann, H. Nakauchi, Z. Ju, H. A. Kestler, L. Zender, K. L. Rudolph, A differentiation checkpoint limits hematopoietic stem cell self-renewal in response to DNA damage. *Cell* **148**, 1001–1014 (2012).
25. B. M. Moehrle, K. Nattamai, A. Brown, M. C. Florian, M. Ryan, M. Vogel, C. Bliederhaeuser, K. Soller, D. R. Prows, A. Abdollahi, D. Schleimer, D. Walter, M. D. Milsom, P. Stambrook, M. Porteus, H. Geiger, Stem cell–specific mechanisms ensure genomic fidelity within HSCs and upon aging of HSCs. *Cell Rep.* **13**, 2412–2424 (2015).
26. M. Mohrin, E. Bourke, D. Alexander, M. R. Warr, K. Barry-Holson, M. M. Le Beau, C. G. Morrison, E. Passegué, Hematopoietic stem cell quiescence promotes error-prone DNA repair and mutagenesis. *Cell Stem Cell* **7**, 174–185 (2010).
27. M. C. Gundry, L. Brunetti, A. Lin, A. E. Mayle, A. Kitano, D. Wagner, J. I. Hsu, K. A. Hoegenauer, C. M. Rooney, M. A. Goodell, D. Nakada, Highly efficient genome editing of murine and human hematopoietic progenitor cells by CRISPR/Cas9. *Cell Rep.* **17**, 1453–1461 (2016).
28. R. J. Platt, S. Chen, Y. Zhou, M. J. Yim, L. Swiech, H. R. Kempton, J. E. Dahlman, O. Parnas, T. M. Eisenhaure, M. Jovanovic, D. B. Graham, S. Jhunjhunwala, M. Heidenreich, R. J. Xavier, R. Langer, D. G. Anderson, N. Hacohen, A. Regev, G. Feng, P. A. Sharp, F. Zhang, CRISPR-Cas9 knockin mice for genome editing and cancer modeling. *Cell* **159**, 440–455 (2014).
29. S. Q. Tsai, Z. Zheng, N. T. Nguyen, M. Liebers, V. V. Topkar, V. Thapar, N. Wyvekens, C. Khayter, A. J. Iafrate, L. P. Le, M. J. Aryee, J. K. Joung, GUIDE-seq enables genome-wide profiling of off-target cleavage by CRISPR-Cas nucleases. *Nat. Biotechnol.* **33**, 187–197 (2015).
30. A. Lombardo, D. Cesana, P. Genovese, B. Di Stefano, E. Provasi, D. F. Colombo, M. Neri, Z. Magnani, A. Cantore, P. Lo Riso, M. Damo, O. M. Pello, M. C. Holmes, P. D. Gregory, A. Gritti, V. Broccoli, C. Bonini, L. Naldini, Site-specific integration and tailoring of cassette design for sustainable gene transfer. *Nat. Methods* **8**, 861–869 (2011).
31. S. S. De Ravin, X. Wu, S. Moir, S. Anaya-O'Brien, N. Kwatemaa, P. Littel, N. Theobald, U. Choi, L. Su, M. Marquesen, D. Hilligoss, J. Lee, C. M. Buckner, K. A. Zarember, G. O'Connor, D. McVicar, D. Kuhns, R. E. Throm, S. Zhou, L. D. Notarangelo, I. C. Hanson, M. J. Cowan, E. Kang, C. Hadigan, M. Meagher, J. T. Gray, B. P. Sorrentino, H. L. Malech, Lentiviral hematopoietic stem cell gene therapy for X-linked severe combined immunodeficiency. *Sci. Transl. Med.* **8**, 335ra57 (2016).
32. S. L. Ginn, C. V. Hallwirth, S. H. Y. Liao, E. T. Teber, J. W. Arthur, J. Wu, H. C. Lee, S. S. Tay, M. Hu, R. R. Reddel, M. P. McCormack, A. J. Thrasher, M. Cavazzana, S. I. Alexander, I. E. Alexander, Limiting thymic precursor supply increases the risk of lymphoid malignancy in murine X-linked severe combined immunodeficiency. *Mol. Ther. Nucleic Acids* **6**, 1–14 (2017).
33. S. Hacein-Bey-Abina, A. Garrigue, G. P. Wang, J. Soulier, A. Lim, E. Morillon, E. Clappier, L. Caccavelli, E. Delabesse, K. Beldjord, V. Asnafi, E. MacIntyre, L. Dal Cortivo, I. Radford, N. Brousse, F. Sigaux, D. Moshous, J. Hauer, A. Borkhardt, B. H. Belohradsky, U. Wintergerst, M. C. Velez, L. Leiva, R. Sorensen, N. Wulffraat, S. Blanche, F. D. Bushman, A. Fischer, M. Cavazzana-Calvo, Insertional oncogenesis in 4 patients after retrovirus-mediated gene therapy of SCID-X1. *J. Clin. Invest.* **118**, 3132–3142 (2008).
34. M. Lo, M. L. Bloom, K. Imada, M. Berg, J. M. Bollenbacher, E. T. Bloom, B. L. Kelsall, W. J. Leonard, Restoration of lymphoid populations in a murine model of X-linked severe combined immunodeficiency by a gene-therapy approach. *Blood* **94**, 3027–3036 (1999).
35. S. Zhou, D. Mody, S. S. DeRavin, J. Hauer, T. Lu, Z. Ma, S. Hacein-Bey Abina, J. T. Gray, M. R. Greene, M. Cavazzana-Calvo, H. L. Malech, B. P. Sorrentino, A self-inactivating lentiviral vector for SCID-X1 gene therapy that does not activate LMO2 expression in human T cells. *Blood* **116**, 900–908 (2010).
36. L. Naldini, Gene therapy returns to centre stage. *Nature* **526**, 351–360 (2015).
37. K. Kariko, H. Muramatsu, J. Ludwig, D. Weissman, Generating the optimal mRNA for therapy: HPLC purification eliminates immune activation and improves translation of nucleoside-modified, protein-encoding mRNA. *Nucleic Acids Res.* **39**, e142 (2011).
38. P. D. Hsu, D. A. Scott, J. A. Weinstein, F. A. Ran, S. Konermann, V. Agarwala, Y. Li, E. J. Fine, X. Wu, O. Shalem, T. J. Cradick, L. A. Marraffini, G. Bao, F. Zhang, DNA targeting specificity of RNA-guided Cas9 nucleases. *Nat. Biotechnol.* **31**, 827–832 (2013).
39. A. Capotondo, R. Milazzo, L. S. Politi, A. Quattrini, A. Palini, T. Plati, S. Merella, A. Nonis, C. di Serio, E. Montini, L. Naldini, A. Biffi, Brain conditioning is instrumental for successful microglia reconstitution following hematopoietic stem cell transplantation. *Proc. Natl. Acad. Sci. U.S.A.* **109**, 15018–15023 (2012).
40. M. Bosticardo, E. Draghici, F. Schena, A. V. Sauer, E. Fontana, M. C. Castiello, M. Catucci, M. Locci, L. Naldini, A. Aiuti, M. G. Roncarolo, P. L. Poliani, E. Traggiai, A. Villa, Lentiviral-mediated gene therapy leads to improvement of B-cell functionality in a murine model of Wiskott-Aldrich syndrome. *J. Allergy Clin. Immunol.* **127**, 1376–1384. e5 (2011).
41. M. Iannacone, G. Sitia, M. Isogawa, J. K. Whitmire, P. Marchese, F. V. Chisari, Z. M. Ruggeri, L. G. Guidotti, Platelets prevent IFN-α/β-induced lethal hemorrhage promoting CTL-dependent clearance of lymphocytic choriomeningitis virus. *Proc. Natl. Acad. Sci. U.S.A.* **105**, 629–634 (2008).
42. E. Provasi, P. Genovese, A. Lombardo, Z. Magnani, P.-Q. Liu, A. Reik, V. Chu, D. E. Paschon, L. Zhang, J. Kuball, B. Camisa, A. Bondanza, G. Casorati, M. Ponzoni, F. Ciceri, C. Bordignon, P. D. Greenberg, M. C. Holmes, P. D. Gregory, L. Naldini, C. Bonini, Editing T cell specificity towards leukemia by zinc finger nucleases and lentiviral gene transfer. *Nat. Med.* **18**, 807–815 (2012).
43. B. L. Oakes, D. F. Xia, E. F. Rowland, D. J. Xu, I. Ankoudinova, J. S. Borchardt, L. Zhang, P. Li, J. C. Miller, E. J. Rebar, M. B. Noyes, Multi-reporter selection for the design of active and more specific zinc-finger nucleases for genome editing. *Nat. Commun.* **7**, 10194 (2016).

Acknowledgments: We thank the Naldini laboratory; D. Canarutto and A. Capotondo for discussion; T. Di Tomaso, A. Ranghetti, P. Di Lucia, and M. Rocchi for technical help; A. Migliara and P. Capasso for providing gRNA plasmids; E. Giuliani for HPLC purification; the San Raffaele flow cytometry facility; and F. Cugnata and C. Di Serio of the University Center for Statistics in Biomedical Sciences for assistance with statistical analyses. **Funding:** This work was supported by grants to L.N. from Telethon (TIGET grant D2 2011-15, TIGET grant E1 2016), the European Union (FP7 601958 SUPERSIST), and the Italian Ministry of Health (NET-2011-02350069) and to P.G. from Telethon (TIGET grant E3 2016) and the Italian Ministry of Health (GR-2013-02358956). **Author contributions:** G. Schiroli designed the experiments, performed the research, interpreted the data, and wrote the manuscript.

S.F., V.C., A.J., M.C.C., L.A., and T.P. performed the research and interpreted the data. A.C. performed the ZFN optimization and specificity studies. F.S. performed the pathology analyses. A.R.G. provided SCID-X1 patient cells. C.B. provided the purified RNA. R.P. and D.T.S. provided the advice on biological conditioning. M.C.H. provided the ZFNs, interpreted the data, and edited the manuscript. A.V. supervised SCID-X1 mouse characterization. G. Sitia supervised the LCMV infection studies. A.L. contributed to the experimental design. P.G. and L.N. designed and supervised the research, interpreted the data, and wrote the manuscript. L.N. coordinated the study. **Competing interests:** A.C. and M.C.H. are employees of Sangamo Therapeutics. C.B. is an employee of MolMed S.p.A. R.P. is currently an employee of Magenta Therapeutics. L.N. and D.T.S. are cofounders, consultants, and stockholders of Magenta Therapeutics. All other authors declare that they have no competing interests. **Data and materials availability:** The reagents described in this article are available under a material transfer agreement with Ospedale San Raffaele and Fondazione Telethon; requests for materials should be addressed to L.N. and P.G. The ZFN reagents are owned by Sangamo Therapeutics; requests for ZFN reagents should be directed to M.C.H.

Submitted 1 March 2017
Resubmitted 26 June 2017
Accepted 12 September 2017
Published 11 October 2017
10.1126/scitranslmed.aan0820

Citation: G. Schiroli, S. Ferrari, A. Conway, A. Jacob, V. Capo, L. Albano, T. Plati, M. C. Castiello, F. Sanvito, A. R. Gennery, C. Bovolenta, R. Palchaudhuri, D. T. Scadden, M. C. Holmes, A. Villa, G. Sitia, A. Lombardo, P. Genovese, L. Naldini, Preclinical modeling highlights the therapeutic potential of hematopoietic stem cell gene editing for correction of SCID-X1. *Sci. Transl. Med.* **9**, eaan0820 (2017).

Science Translational Medicine

Preclinical modeling highlights the therapeutic potential of hematopoietic stem cell gene editing for correction of SCID-X1

Giulia Schiroli, Samuele Ferrari, Anthony Conway, Aurelien Jacob, Valentina Capo, Luisa Albano, Tiziana Plati, Maria C. Castiello, Francesca Sanvito, Andrew R. Gennery, Chiara Bovolenta, Rahul Palchaudhuri, David T. Scadden, Michael C. Holmes, Anna Villa, Giovanni Sitia, Angelo Lombardo, Pietro Genovese and Luigi Naldini

Sci Transl Med **9**, eaan0820.
DOI: 10.1126/scitranslmed.aan0820

Gene correction, one step at a time

Although gene therapy has been proposed for a variety of genetic disorders, including severe combined immunodeficiency, it has not yet found routine use in the clinic, in part because of potential complications. To help pave the way for safer translation of such gene therapy, Schiroli *et al*. studied potential approaches to it in mouse models of severe combined immunodeficiency. The authors systematically analyzed the outcomes of using different approaches to conditioning, different numbers of gene-edited cells, different techniques for editing the faulty gene, and other aspects of the technology to find the safest and most effective method.